



**HAL**  
open science

## The latest HyPe(r) in plant H<sub>2</sub>O<sub>2</sub> biosensing

José Manuel Ugalde, Michelle Schlösser, Armelle Dongois, Alexandre Martinière, Andreas Meyer

► **To cite this version:**

José Manuel Ugalde, Michelle Schlösser, Armelle Dongois, Alexandre Martinière, Andreas Meyer.  
The latest HyPe(r) in plant H<sub>2</sub>O<sub>2</sub> biosensing. *Plant Physiology*, 2021, 187 (2), pp.480-484.  
10.1093/plphys/kiab306 . hal-03375961

**HAL Id: hal-03375961**

**<https://hal.science/hal-03375961>**

Submitted on 19 Oct 2021

**HAL** is a multi-disciplinary open access archive for the deposit and dissemination of scientific research documents, whether they are published or not. The documents may come from teaching and research institutions in France or abroad, or from public or private research centers.

L'archive ouverte pluridisciplinaire **HAL**, est destinée au dépôt et à la diffusion de documents scientifiques de niveau recherche, publiés ou non, émanant des établissements d'enseignement et de recherche français ou étrangers, des laboratoires publics ou privés.

# 1 The latest HyPe(r) in plant H<sub>2</sub>O<sub>2</sub> biosensing

2

3 Dear Editor,

4 Hydrogen peroxide (H<sub>2</sub>O<sub>2</sub>) is widely used as a signaling molecule in plants during development,  
5 wounding, pathogen or symbiotic interaction and a wide range of abiotic stresses (Waszczak et al.,  
6 2018; Smirnof and Arnaud, 2019). For better understanding its role as a messenger, it is critical to  
7 measure H<sub>2</sub>O<sub>2</sub> with high spatial and temporal resolution (Gilroy et al., 2016). Stress-induced oxidation  
8 has frequently been shown with oxidation-sensitive fluorescent chemical probes, most prominently  
9 2',7'-dihydrodichlorofluorescein diacetate (Fichman et al., 2019). These probes, however, have the  
10 disadvantage of limited specificity for H<sub>2</sub>O<sub>2</sub> and the fact that they may report only the accumulation of  
11 oxidants over time without any dynamic and spatial information (Winterbourn, 2014; Ortega-  
12 Villasante et al., 2018). In addition, these probes need to be loaded into the cells, where they need to  
13 be deesterified to become active, and they can be analyzed only intensimetrically with excitation at  
14 a single wavelength. Altogether, this renders the observed fluorescence sensitive to several non-  
15 controlled factors and thus often ambiguous. Genetically encoded probes for H<sub>2</sub>O<sub>2</sub> have the promise  
16 of overcoming these limitations (Meyer and Dick, 2010; Schwarzländer et al., 2016). Probes of the  
17 HyPer family consist of a circularly-permuted yellow fluorescent protein (cpYFP) core and a sensing  
18 domain constructed from the bacterial H<sub>2</sub>O<sub>2</sub>-sensitive transcription factor OxyR (Belousov et al., 2006;  
19 Bilan and Belousov, 2016). cpYFP, however, has the disadvantage of a pronounced pH-sensitivity  
20 (Schwarzländer et al., 2014). With a more alkaline cytosolic pH in illuminated green tissues as  
21 measured with cpYFP, HyPer readouts of H<sub>2</sub>O<sub>2</sub> fluxes become highly ambiguous and demand elaborate  
22 controls (Exposito-Rodriguez et al., 2017). In contrast, roGFP2-Orp1 is pH-insensitive and has  
23 successfully been used to sense H<sub>2</sub>O<sub>2</sub> originating from an elicitor-induced oxidative burst in the  
24 apoplast and from chloroplasts in which ROS production was boosted by methyl viologen (MV) in  
25 combination with light (Nietzel et al., 2019; Ugalde et al., 2021). Small dynamic changes in H<sub>2</sub>O<sub>2</sub> in the  
26 low nanomolar range may, however, not be easily detectable because of a limited responsiveness of  
27 Orp1 to H<sub>2</sub>O<sub>2</sub> and it may be overridden by a strong reducing effect of glutathione. Indeed, mutants  
28 with a less negative glutathione redox potential ( $E_{GSH}$ ) render the sensor more responsive due to the  
29 diminished reducing power (Marty et al., 2009; Nietzel et al., 2019).

30 Recently, a novel ultrasensitive HyPer variant, HyPer7, consisting of the OxyR protein of *Neisseria*  
31 *meningitidis* and a mutated cpYFP, which in contrast to its earlier versions is largely pH-insensitive, was  
32 reported (Pak et al., 2020). These features sparked much interest across biology and thus we are  
33 currently observing multiple laboratories considering the use of HyPer7. To test its ability for reporting  
34 dynamic changes of H<sub>2</sub>O<sub>2</sub> in the cytosol of *Arabidopsis thaliana*, we generated stable HyPer7 reporter  
35 lines. These plants did not show any obvious phenotype (Supplemental Materials and Methods;  
36 Supplemental Fig. S1). Ratiometric analysis of HyPer7 indicated that the sensor was largely reduced in  
37 all tissues except the root meristem, where HyPer7 appeared slightly oxidized (Supplemental Figs. S1  
38 and S7). Depletion of glutathione by germinating seeds on L-buthionine sulfoximine (BSO) (Meyer et  
39 al., 2007) did cause only a slight ratio increase in HyPer7 while the original HyPer (Costa et al., 2010)  
40 was unresponsive and roGFP2-Orp1 (Nietzel et al., 2019) was fully oxidized (Supplemental Fig. S2). This  
41 suggests that reduction of HyPer7 is largely independent of  $E_{GSH}$ , but that with GSH depletion, H<sub>2</sub>O<sub>2</sub>  
42 increase to levels that can be sensed by HyPer7. To further elucidate the responsiveness of HyPer7 to  
43 an externally imposed oxidation, we perfused seedlings with H<sub>2</sub>O<sub>2</sub>, buffer and DTT and compared its  
44 response with reporter lines expressing roGFP2-Orp1 and HyPer (Supplemental Materials and  
45 Methods; Fig. 1A). When perfused with H<sub>2</sub>O<sub>2</sub>, all three sensors showed a concentration-dependent  
46 increase of the fluorescence ratio with HyPer7 showing the largest fold-change of about 4 compared

47 to 3.2 for roGFP2-Orp1 and less than 2 for HyPer with 1 mM H<sub>2</sub>O<sub>2</sub> perfusion (Fig. 1B-D). The speed of  
48 oxidation of HyPer7 after perfusion with H<sub>2</sub>O<sub>2</sub> was slightly faster than for the other sensors. Cytosolic  
49 changes in H<sub>2</sub>O<sub>2</sub> after perfusion with 0.01 mM H<sub>2</sub>O<sub>2</sub> were only visible with HyPer7 (Fig. 1E-G).  
50 Subsequent perfusion with buffer consistently led to a decline in the fluorescence ratio. Addition of 10  
51 mM DTT 6 minutes after the washout of H<sub>2</sub>O<sub>2</sub> caused a further drop in ratio back to the starting value  
52 for roGFP2-Orp1 consistent with the response of other roGFP2-based probes (Marty et al., 2009), but  
53 did not cause any distinct change for HyPer7 (Fig. 1B-D; Supplemental Fig. S3A). This suggests that DTT  
54 is not capable of efficiently reducing the OxyR domain. Consistent with this observation, 10 mM DTT  
55 exerted only a minor reducing effect on recombinant HyPer7 while 5 mM of the stronger reductant  
56 Tris(2-carboxyethyl)phosphine hydrochloride (TCEP) reduced the protein completely (Supplemental  
57 Fig. S3B).

58 Direct comparison of HyPer and HyPer7 for their response to externally added H<sub>2</sub>O<sub>2</sub> in roots  
59 consistently showed the more pronounced response of HyPer7 (Supplemental Fig. S4). While HyPer  
60 showed an oxidation response to 10 mM H<sub>2</sub>O<sub>2</sub> in leaves, the same H<sub>2</sub>O<sub>2</sub> concentration did not cause a  
61 ratio increase in roots, or even caused a complete lack of excitability at 488 nm preventing any  
62 ratiometric analysis. A pronounced drop in the fluorescence ratio of cpYFP with H<sub>2</sub>O<sub>2</sub> identifies the  
63 decrease of the HyPer ratio to be caused by H<sub>2</sub>O<sub>2</sub>-induced acidosis in the cytosol (Supplemental Fig.  
64 S5). pH-clamp experiments on roots showed the pronounced pH-dependence of HyPer while HyPer7  
65 is largely pH-independent at neutral and slightly alkaline pH (Supplemental Fig. S6). This pH-  
66 insensitivity of HyPer7 avoids ambiguities in the interpretation of measured ratio values.

67 To explore the capability of HyPer7 for sensing stress-induced H<sub>2</sub>O<sub>2</sub> in live plant cells, we tested the  
68 response to different stress factors. In roots, addition of 100 mM NaCl caused a slight oxidation in the  
69 meristematic zone, but not in the elongation zone (Supplemental Fig. S7). In leaves, 50 μM MV in  
70 combination with light causes the formation of H<sub>2</sub>O<sub>2</sub>, which is detectable with roGFP2-based probes  
71 (Ugalde et al., 2021). The response of HyPer7 suggests that HyPer7 is more sensitive than roGFP2-Orp1  
72 and that 50 μM MV already resulted in a pronounced cytosolic oxidation with the normal plate reader  
73 excitation light (Supplemental Fig. S8A). Continuous illumination with actinic light for 1 h caused a  
74 strong oxidation, which quickly disappeared after the illumination period. Similarly, roGFP2-Orp1 can  
75 be used to monitor the cytosolic response to an apoplastic oxidative burst elicited by flg22 (Nietzel et  
76 al., 2019). While HyPer under the conditions used was not sensitive enough to monitor this burst, the  
77 response of HyPer7 was more pronounced than that of roGFP2-Orp1 (Supplemental Fig. S8B). The  
78 response of HyPer7 also indicated an additional, yet to be characterized, earlier oxidation peak about  
79 30 min after addition of flg22, which was not observed with roGFP2-Orp1. HyPer7 thus may allow to  
80 generate information that complements previous findings.

81 In pavement cells of cotyledons, illumination by laser light during scanning already caused a gradual  
82 oxidation of HyPer7, which increases depending on the zoom factor (Fig. 2; Supplemental Fig. S9).  
83 Surprisingly, this oxidation was almost completely abolished when seedlings were pretreated with 20  
84 μM DCMU as an inhibitor of photosynthetic electron transport (Fig. 2B, D, E). These results, suggests  
85 that laser light used for excitation is sufficient to induce H<sub>2</sub>O<sub>2</sub>-release from chloroplasts, and that these  
86 low amounts of H<sub>2</sub>O<sub>2</sub> can be detected by HyPer7. Laser-induced oxidation of HyPer declined within  
87 minutes indicated by a decreasing fluorescence ratio (Fig. 2F-H). The capability of sequentially  
88 repeating this oxidation-reduction cycle emphasizes the dynamic response of HyPer7 albeit with a  
89 slower reduction phase.

90 In summary, the results show that HyPer7 is largely pH-insensitive and more sensitive to H<sub>2</sub>O<sub>2</sub> than  
91 current probes. Nonetheless, the Arabidopsis cytosol appears to lack an efficient reduction system for  
92 HyPer7, which may limit its use for fully dynamic studies. With an increased sensitivity, HyPer7 offers  
93 the possibility of detecting physiological H<sub>2</sub>O<sub>2</sub> fluxes and thus opens the door for further studies on

94 intracellular H<sub>2</sub>O<sub>2</sub> signaling during normal development and under environmental stress. At the same  
95 time the high sensitivity, at least in green tissues, bears the risk of generating artefacts if non-  
96 photosynthesis-related H<sub>2</sub>O<sub>2</sub> signaling processes are to be investigated. Knowing these potential  
97 artefacts should help designing appropriate control experiments and with that generate data that help  
98 elucidating H<sub>2</sub>O<sub>2</sub> signaling.

99

## 100 **Supplemental Data**

101 The following supplemental materials are available:

102 **Supplemental Figure S1.** Expression of the HyPer7 sensor in *Arabidopsis thaliana*.

103 **Supplemental Figure S2.** Effect of GSH depletion on the oxidation of genetically encoded H<sub>2</sub>O<sub>2</sub> probes.

104 **Supplemental Figure S3.** Excitation spectra of HyPer7 *in vivo* and *in vitro*.

105 **Supplemental Figure S4.** Determination of minimum and maximum oxidation of different H<sub>2</sub>O<sub>2</sub> probes.

106 **Supplemental Figure S5.** Hydrogen peroxide causes acidification in the cytosol.

107 **Supplemental Figure S6.** Response of HyPer and HyPer7 to changes in intracellular pH.

108 **Supplemental Figure S7.** HyPer7 ratio changes in root cells treated with salt.

109 **Supplemental Figure S8.** Methyl viologen (MV)-induced photo-oxidative stress and the elicitor flg22  
110 causes oxidation of H<sub>2</sub>O<sub>2</sub> probes in the cytosol.

111 **Supplemental Figure S9.** Oxidation of HyPer7 depends on laser light intensity reaching the scanned  
112 area.

113 **Supplemental Materials and Methods.** Methodology used in this study

114

## 115 **ACKNOWLEDGEMENTS**

116 We thank Dr. Vsevolod Belousov for providing the HyPer7 construct and Dr. Alex Costa for providing  
117 *Arabidopsis* seeds with expression of HyPer in the cytosol. We are grateful to Maria Homagk for  
118 excellent technical assistance and Markus Schwarzländer for continuous discussion. We thank the  
119 Montpellier Ressources Imagerie (MRI) and the Histocytology and Plant Cell Imaging Platform for  
120 providing the microscope facility (PHIV).

121

## 122 **Author contributions**

123 A.J.M., A.M., A.D. and J.M.U. designed experiments and analyzed data; M.S., A.D., A.M. and J.M.U.  
124 performed experiments; A.J.M. and A.M. supervised experiments; A.J.M. wrote the article.

125

## 126 **Funding information**

127 This work was funded by the Deutsche Forschungsgemeinschaft (DFG) within the framework of the  
128 Priority Program SPP1710 “Dynamics of thiol-based redox switches in cellular physiology” (ME1567/9-

129 2; AJM) and the DAAD-PROCOPE project 57561426 (AJM and AM). A.M. is also funded by the Agence  
130 National de la Recherche (ANR) CelloSmo (ANR-19-CE20-0008-01).

131

## 132 **Authors**

133 José Manuel Ugalde<sup>1</sup>, Michelle Schlößer<sup>1</sup>, Armelle Dongois<sup>2</sup>, Alexandre Martinière<sup>2</sup>, Andreas J.  
134 Meyer<sup>1,3,4</sup>

135 <sup>1</sup>INRES-Chemical Signalling, University of Bonn, Friedrich-Ebert-Allee 144, 53113 Bonn, Germany

136 <sup>2</sup>BPMP, Univ Montpellier, CNRS, INRAE, Institut Agro, Montpellier, France

137

138 <sup>3</sup>senior author

139

140 <sup>4</sup>Author for correspondence: andres.meyer@uni-bonn.de

141

## 142 **ORCID IDs**

143 JMU: 0000-0002-0601-4302

144 MS: 0000-0001-6913-8356

145 AD: 0000-0002-3911-4203

146 AM: 0000-0003-0663-6854

147 AJM: 0000-0001-8144-4364

148

## 149 **LITERATURE CITED**

150 **Belousov VV, Fradkov AF, Lukyanov KA, Staroverov DB, Shakhbazov KS, Terskikh AV, Lukyanov S**  
151 (2006) Genetically encoded fluorescent indicator for intracellular hydrogen peroxide. *Nat*  
152 *Methods* **3**: 281–286

153 **Bilan DS, Belousov VV** (2016) HyPer family probes: state of the art. *Antioxid Redox Signal* **24**: 731–  
154 751

155 **Costa A, Drago I, Behera S, Zottini M, Pizzo P, Schroeder JI, Pozzan T, Lo Schiavo F** (2010) H<sub>2</sub>O<sub>2</sub> in  
156 plant peroxisomes: an *in vivo* analysis uncovers a Ca<sup>2+</sup>-dependent scavenging system. *Plant J*  
157 **62**: 760–772

158 **Exposito-Rodriguez M, Laissue PP, Yvon-Durocher G, Smirnov N, Mullineaux PM** (2017)  
159 Photosynthesis-dependent H<sub>2</sub>O<sub>2</sub> transfer from chloroplasts to nuclei provides a high-light  
160 signalling mechanism. *Nat Commun* **8**: 49

161 **Fichman Y, Miller G, Mittler R** (2019) Whole-plant live imaging of reactive oxygen species. *Mol Plant*  
162 **12**: 1203–1210

- 163 **Gilroy S, Białasek M, Suzuki N, Górecka M, Devireddy AR, Karpiński S, Mittler R** (2016) ROS, calcium,  
164 and electric signals: key mediators of rapid systemic signaling in plants. *Plant Physiol* **171**:  
165 1606–1615
- 166 **Marty L, Siala W, Schwarzländer M, Fricker MD, Wirtz M, Sweetlove LJ, Meyer Y, Meyer AJ,**  
167 **Reichheld J-P, Hell R** (2009) The NADPH-dependent thioredoxin system constitutes a  
168 functional backup for cytosolic glutathione reductase in *Arabidopsis*. *Proc Natl Acad Sci USA*  
169 **106**: 9109–9114
- 170 **Meyer AJ, Brach T, Marty L, Kreye S, Rouhier N, Jacquot J-P, Hell R** (2007) Redox-sensitive GFP in  
171 *Arabidopsis thaliana* is a quantitative biosensor for the redox potential of the cellular  
172 glutathione redox buffer. *Plant J* **52**: 973–986
- 173 **Meyer AJ, Dick TP** (2010) Fluorescent protein-based redox probes. *Antioxid Redox Signal* **13**: 621–  
174 650
- 175 **Nietzel T, Elsässer M, Ruberti C, Steinbeck J, Ugalde JM, Fuchs P, Wagner S, Ostermann L, Moseler**  
176 **A, Lemke P, et al** (2019) The fluorescent protein sensor roGFP2-Orp1 monitors *in vivo* H<sub>2</sub>O<sub>2</sub>  
177 and thiol redox integration and elucidates intracellular H<sub>2</sub>O<sub>2</sub> dynamics during elicitor-induced  
178 oxidative burst in *Arabidopsis*. *New Phytol* **221**: 1649–1664
- 179 **Ortega-Villasante C, Burén S, Blázquez-Castro A, Barón-Sola Á, Hernández LE** (2018) Fluorescent *in*  
180 *vivo* imaging of reactive oxygen species and redox potential in plants. *Free Radic Biol Med*  
181 **122**: 202–220
- 182 **Pak VV, Ezeriņa D, Lyublinskaya OG, Pedre B, Tyurin-Kuzmin PA, Mishina NM, Thauvin M, Young D,**  
183 **Wahni K, Gache SAM, et al** (2020) Ultrasensitive genetically encoded indicator for hydrogen  
184 peroxide identifies roles for the oxidant in cell migration and mitochondrial function. *Cell*  
185 *Metab* **31**: 642–653.e6
- 186 **Schwarzländer M, Dick TP, Meyer AJ, Morgan B** (2016) Dissecting redox biology using fluorescent  
187 protein sensors. *Antioxid Redox Signal* **24**: 680–712
- 188 **Schwarzländer M, Wagner S, Ermakova YG, Belousov VV, Radi R, Beckman JS, Buettner GR,**  
189 **Demaurex N, Duchon MR, Forman HJ, et al** (2014) The “mitoflash” probe cpYFP does not  
190 respond to superoxide. *Nature* **514**: E12–14
- 191 **Smirnov N, Arnaud D** (2019) Hydrogen peroxide metabolism and functions in plants. *New Phytol*  
192 **221**: 1197–1214
- 193 **Ugalde JM, Fuchs P, Nietzel T, Cutolo EA, Homagk M, Vothknecht UC, Holuigue L, Schwarzländer M,**  
194 **Müller-Schüssele SJ, Meyer AJ** (2021) Chloroplast-derived photo-oxidative stress causes  
195 changes in H<sub>2</sub>O<sub>2</sub> and E<sub>GSH</sub> in other subcellular compartments. *Plant Physiol*. doi:  
196 10.1093/plphys/kiaa095
- 197 **Waszczak C, Carmody M, Kangasjärvi J** (2018) Reactive oxygen species in plant signaling. *Annu Rev*  
198 *Plant Biol* **69**: 209–236
- 199 **Winterbourn CC** (2014) The challenges of using fluorescent probes to detect and quantify specific  
200 reactive oxygen species in living cells. *Biochim Biophys Acta* **1840**: 730–738

201 **Figure Legends**

202 **Figure 1.** Oxidation and reduction of different genetically encoded H<sub>2</sub>O<sub>2</sub> probes in the cytosol of wild-  
203 type Arabidopsis seedlings. A, Experimental design for sequential perfusion with different  
204 concentrations of H<sub>2</sub>O<sub>2</sub>, imaging buffer and 10 mM DTT. B, Confocal microscopy images of root cells  
205 from 7-day-old seedlings expressing HyPer7, HyPer or roGFP2-Orp1, all targeted to the cytosol. The  
206 false color ratio images show the fluorescence ratios calculated from two separate images collected  
207 with excitation at 488 nm and 405 nm. Emission was collected at 508-535 nm. Ratios are 488 nm/ 405  
208 nm for HyPer7 and HyPer, and 405 nm/488 nm for roGFP2-Orp1. Bar, 50 μm. C, D, Typical time courses  
209 showing the dynamic response of the probes to transient oxidation by the indicated H<sub>2</sub>O<sub>2</sub> treatments  
210 (arrows). All ratios are normalized to the starting values at t = 0 min. n = 3–4 replicates. E–G, Slopes of  
211 the ratio value changes after H<sub>2</sub>O<sub>2</sub> perfusion in the indicated concentrations. The slopes were  
212 calculated from ratio values between 3.9–4.7 min. Data indicates the mean values ± SD. n = 2–4  
213 replicates.

214

215 **Figure 2.** Laser illumination of green tissues during scanning is sufficient to produce release of H<sub>2</sub>O<sub>2</sub>  
216 from chloroplasts. A, B, Laser-induced oxidation is more visible in cells expressing HyPer7 compared to  
217 cells with HyPer or roGFP2-Orp1. Plants expressing cpYFP were included to test for putative  
218 concomitant pH changes. The false color ratio images show the fluorescence ratios calculated from  
219 two separate images collected with excitation at 488 nm and 405 nm. Emission was collected at 508-  
220 535 nm. Ratios are 488 nm/ 405 nm for HyPer7, HyPer and cpYFP, and 405 nm/488 nm for roGFP2-  
221 Orp1. Bar, 20 μm. C, Ratio values of purified recombinant protein imaged with the same instruments  
222 settings as in (A). The protein was reduced with TCEP prior to the measurement. D, E, Inhibition of  
223 photosynthetic electron transport blocks laser induced oxidation of HyPer7 in the cytosol. Seedlings  
224 were incubated in imaging buffer supplemented with 20 μM DCMU for 45 minutes in the dark prior to  
225 the measurement. Bar, 20 μm. F–H, Laser-induced oxidation of HyPer7 in a defined region of interest  
226 (magenta square) is reversible. Letters indicate time windows for laser-induced oxidation caused by  
227 high frequency imaging at high zoom (a-b and c-d) and a recovery phase with intermittent imaging at  
228 low zoom (b-c and d-e). G, Fluorescence measured from the two independent channels (405 nm and  
229 488 nm), normalized to the value at t = 0 min. All ratios in B, C, E and H are normalized to the ratio  
230 value at t = 0 min. Mean ratios + SD , n = 4–11 replicates.

231

232

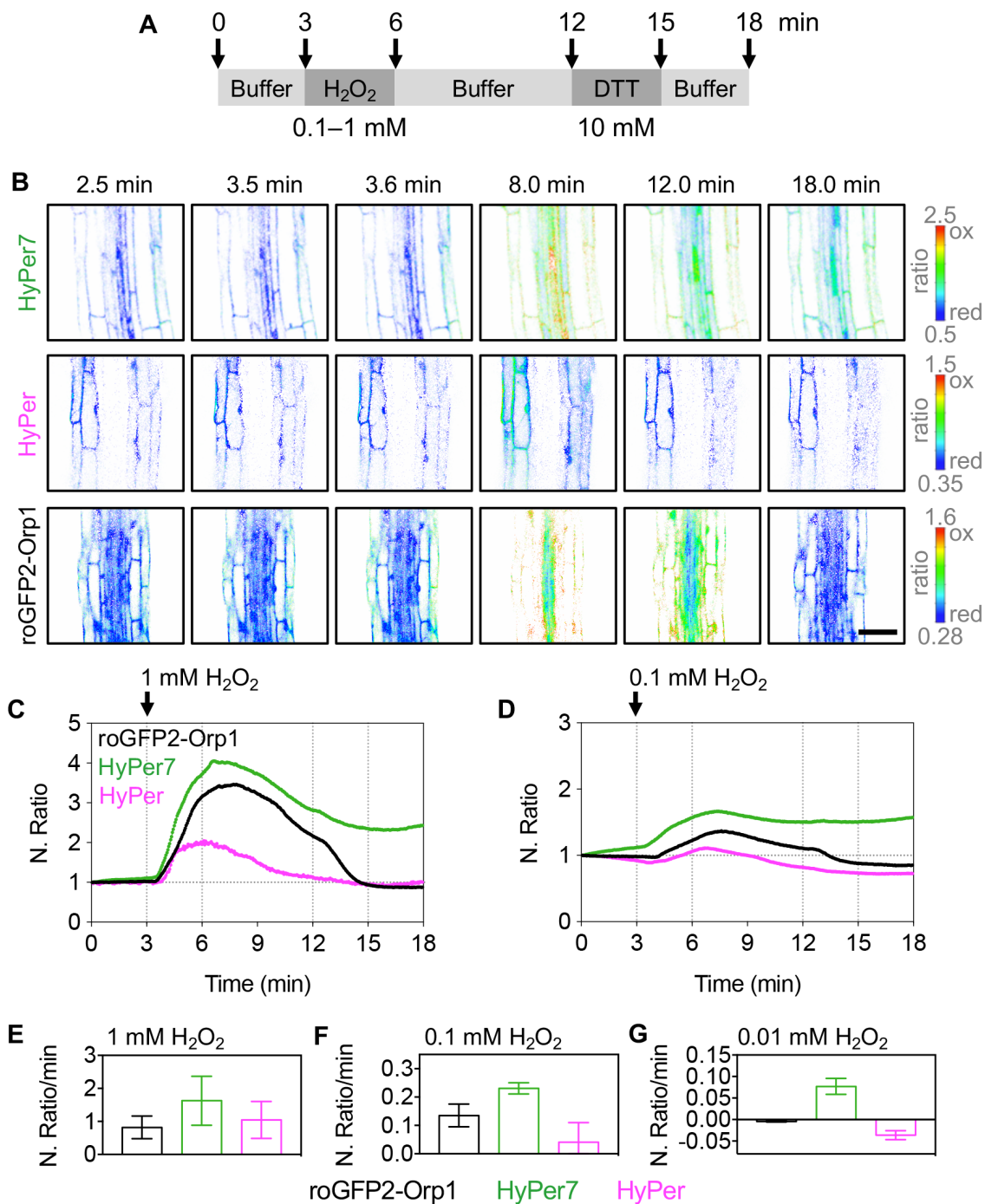


**Figure 1.** Oxidation and reduction of different genetically encoded H<sub>2</sub>O<sub>2</sub> probes in the cytosol of wild-type *Arabidopsis* seedlings. **A**, Experimental design for sequential perfusion with different concentrations of H<sub>2</sub>O<sub>2</sub>, imaging buffer and 10 mM DTT. **B**, Confocal microscopy images of root cells from 7-day-old seedlings expressing HyPer7, HyPer or roGFP2-Orp1, all targeted to the cytosol. The false color ratio images show the fluorescence ratios calculated from two separate images collected with excitation at 488 nm and 405 nm. Emission was collected at 508–535 nm. Ratios are 488 nm/ 405 nm for HyPer7 and HyPer, and 405 nm/488 nm for roGFP2-Orp1. Bar, 50  $\mu$ m. **C**, **D**, Typical time courses showing the dynamic response of the probes to transient oxidation by the indicated H<sub>2</sub>O<sub>2</sub> treatments (arrows). All ratios are normalized to the starting values at t = 0 min. n = 3–4 replicates. **E–G**, Slopes of the ratio value changes after H<sub>2</sub>O<sub>2</sub> perfusion in the indicated concentrations. The slopes were calculated from ratio values between 3.9–4.7 min. Data indicates the mean values  $\pm$  SD. n = 2–4 replicates.



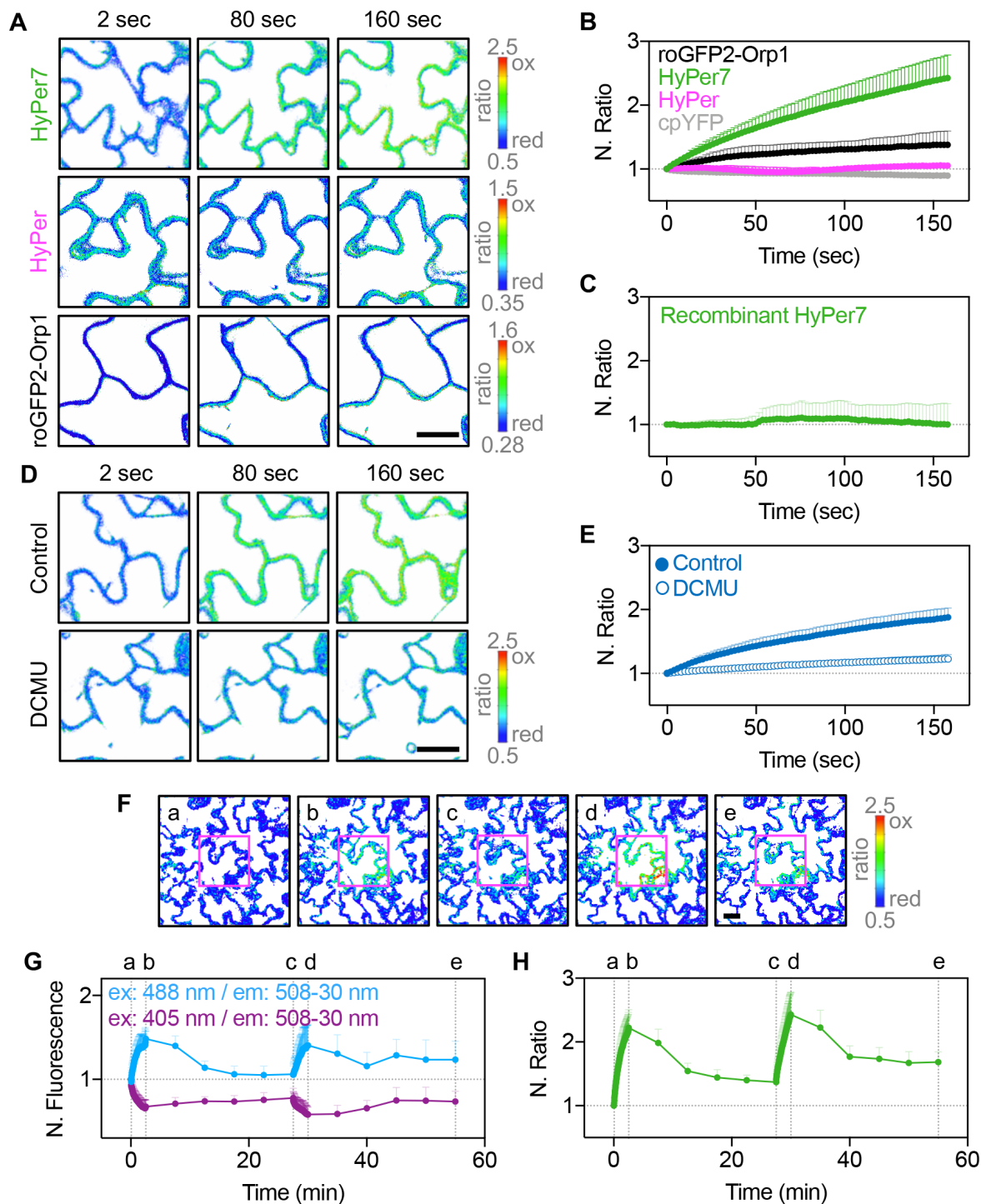


**Figure 2.** Laser illumination of green tissues during scanning is sufficient to produce release of  $H_2O_2$

form chloroplasts. A, B, Laser-induced oxidation is more visible in cells expressing HyPer7 compared to cells with HyPer or roGFP2-Orp1. Plants expressing cpYFP were included to test for putative concomitant pH changes. The false color ratio images show the fluorescence ratios calculated from two separate images collected with excitation at 488 nm and 405 nm. Emission was collected at 508-535 nm. Ratios are 488 nm/ 405 nm for HyPer7, HyPer and cpYFP, and 405 nm/488 nm for roGFP2-Orp1. Bar, 20  $\mu$ m. C, Ratio values of purified recombinant protein imaged with the same instrument settings as in (A). The protein was reduced with TCEP prior to the measurement. D, E, Inhibition of photosynthetic electron transport blocks laser induced oxidation of HyPer7 in the cytosol. Seedlings were incubated in imaging buffer supplemented with 20  $\mu$ M DCMU for 45 minutes in the dark prior to the measurement. Bar, 20  $\mu$ m. F–H, Laser-induced oxidation of HyPer7 in a defined region of interest (magenta square) is reversible. Letters indicate time windows for laser-induced oxidation caused by high frequency imaging at high zoom (a-b and c-d) and a recovery phase with intermittent imaging at low zoom (b-c and d-e).

G, Fluorescence measured from the two independent channels (405 nm and 488 nm), normalized to the value at  $t = 0$  min. All ratios in B, C, E and H are normalized to the ratio value at  $t = 0$  min. Mean ratios + SD,  $n = 4$ –11 replicates.

## Parsed Citations

- Belousov VV, Fradkov AF, Lukyanov KA, Staroverov DB, Shakhbazov KS, Terskikh AV, Lukyanov S (2006) Genetically encoded fluorescent indicator for intracellular hydrogen peroxide. *Nat Methods* 3: 281–286**  
Google Scholar: [Author Only](#) [Title Only](#) [Author and Title](#)
- Bilan DS, Belousov VV (2016) HyPer family probes: state of the art. *Antioxid Redox Signal* 24: 731–751**  
Google Scholar: [Author Only](#) [Title Only](#) [Author and Title](#)
- Costa A, Drago I, Behera S, Zottini M, Pizzo P, Schroeder JI, Pozzan T, Lo Schiavo F (2010) H<sub>2</sub>O<sub>2</sub> in plant peroxisomes: an in vivo analysis uncovers a Ca<sup>2+</sup>-dependent scavenging system. *Plant J* 62: 760–772**  
Google Scholar: [Author Only](#) [Title Only](#) [Author and Title](#)
- Exposito-Rodriguez M, Laissue PP, Yvon-Durocher G, Smirnov N, Mullineaux PM (2017) Photosynthesis-dependent H<sub>2</sub>O<sub>2</sub> transfer from chloroplasts to nuclei provides a high-light signalling mechanism. *Nat Commun* 8: 49**  
Google Scholar: [Author Only](#) [Title Only](#) [Author and Title](#)
- Fichman Y, Miller G, Mittler R (2019) Whole-plant live imaging of reactive oxygen species. *Mol Plant* 12: 1203–1210**  
Google Scholar: [Author Only](#) [Title Only](#) [Author and Title](#)
- Gilroy S, Białasek M, Suzuki N, Górecka M, Devireddy AR, Karpiński S, Mittler R (2016) ROS, calcium, and electric signals: key mediators of rapid systemic signaling in plants. *Plant Physiol* 171: 1606–1615**  
Google Scholar: [Author Only](#) [Title Only](#) [Author and Title](#)
- Marty L, Siala W, Schwarzländer M, Fricker MD, Wirtz M, Sweetlove LJ, Meyer Y, Meyer AJ, Reichheld J-P, Hell R (2009) The NADPH-dependent thioredoxin system constitutes a functional backup for cytosolic glutathione reductase in Arabidopsis. *Proc Natl Acad Sci USA* 106: 9109–9114**  
Google Scholar: [Author Only](#) [Title Only](#) [Author and Title](#)
- Meyer AJ, Brach T, Marty L, Kreye S, Rouhier N, Jacquot J-P, Hell R (2007) Redox-sensitive GFP in Arabidopsis thaliana is a quantitative biosensor for the redox potential of the cellular glutathione redox buffer. *Plant J* 52: 973–986**  
Google Scholar: [Author Only](#) [Title Only](#) [Author and Title](#)
- Meyer AJ, Dick TP (2010) Fluorescent protein-based redox probes. *Antioxid Redox Signal* 13: 621–650**  
Google Scholar: [Author Only](#) [Title Only](#) [Author and Title](#)
- Nietzel T, Elsässer M, Ruberti C, Steinbeck J, Ugalde JM, Fuchs P, Wagner S, Ostermann L, Moseler A, Lemke P, et al (2019) The fluorescent protein sensor roGFP2-Orp1 monitors in vivo H<sub>2</sub>O<sub>2</sub> and thiol redox integration and elucidates intracellular H<sub>2</sub>O<sub>2</sub> dynamics during elicitor-induced oxidative burst in Arabidopsis. *New Phytol* 221: 1649–1664**  
Google Scholar: [Author Only](#) [Title Only](#) [Author and Title](#)
- Ortega-Villasante C, Burén S, Blázquez-Castro A, Barón-Sola Á, Hernández LE (2018) Fluorescent in vivo imaging of reactive oxygen species and redox potential in plants. *Free Radic Biol Med* 122: 202–220**  
Google Scholar: [Author Only](#) [Title Only](#) [Author and Title](#)
- Pak VV, Ezeriņa D, Lyublinskaya OG, Pedre B, Tyurin-Kuzmin PA, Mishina NM, Thauvin M, Young D, Wahni K, Gache SAM, et al (2020) Ultrasensitive genetically encoded indicator for hydrogen peroxide identifies roles for the oxidant in cell migration and mitochondrial function. *Cell Metab* 31: 642-653.e6**  
Google Scholar: [Author Only](#) [Title Only](#) [Author and Title](#)
- Schwarzländer M, Dick TP, Meyer AJ, Morgan B (2016) Dissecting redox biology using fluorescent protein sensors. *Antioxid Redox Signal* 24: 680–712**  
Google Scholar: [Author Only](#) [Title Only](#) [Author and Title](#)
- Schwarzländer M, Wagner S, Ermakova YG, Belousov VV, Radi R, Beckman JS, Buettner GR, Demareux N, Duchon MR, Forman HJ, et al (2014) The "mitoflash" probe cpYFP does not respond to superoxide. *Nature* 514: E12-14**  
Google Scholar: [Author Only](#) [Title Only](#) [Author and Title](#)
- Smirnov N, Arnaud D (2019) Hydrogen peroxide metabolism and functions in plants. *New Phytol* 221: 1197–1214**  
Google Scholar: [Author Only](#) [Title Only](#) [Author and Title](#)
- Ugalde JM, Fuchs P, Nietzel T, Cutolo EA, Homagk M, Vothknecht UC, Holuigue L, Schwarzländer M, Müller-Schüssele SJ, Meyer AJ (2021) Chloroplast-derived photo-oxidative stress causes changes in H<sub>2</sub>O<sub>2</sub> and EGSH in other subcellular compartments. *Plant Physiol*. doi: 10.1093/plphys/kiab095**  
Google Scholar: [Author Only](#) [Title Only](#) [Author and Title](#)
- Waszczak C, Carmody M, Kangasjärvi J (2018) Reactive oxygen species in plant signaling. *Annu Rev Plant Biol* 69: 209–236**  
Google Scholar: [Author Only](#) [Title Only](#) [Author and Title](#)
- Winterbourn CC (2014) The challenges of using fluorescent probes to detect and quantify specific reactive oxygen species in living cells. *Biochim Biophys Acta* 1840: 730–738**  
Google Scholar: [Author Only](#) [Title Only](#) [Author and Title](#)